FOCAL MECHANISM STRESS INVERSIONS IN SOUTHERN CALIFORNIA AND THE STRENGTH OF THE SAN ANDREAS FAULT

John Townend and Mark D. Zoback
Department of Geophysics, Stanford University, Stanford, CA 94305-2215

ABSTRACT

We have investigated the orientation of the axis of maximum horizontal compression, S_{Hmax}, with respect to the San Andreas and associated faults in southern California using focal mechanism stress inversion. Our analysis differs from that of previous workers in that we use a data-based recursive gridding algorithm to group focal mechanisms before inversion. This procedure produces a grid whose density mimics that of the local seismicity, and enables us to place more confidence in the necessary assumption of stress homogeneity in those areas where there are numerous data.

In the vicinity of the Big Bend, Mojave Desert, and Joshua Tree–Landers–Big Bear regions we find (1) a high degree of consistency between S_{Hmax} orientations in adjacent grid cells, (2) systematically high angles (>60°) between the orientation of S_{Hmax} and the local strike of major faults, and (3) no consistent rotation of S_{Hmax} near major faults on a scale of ~5 km.

These results agree with S_{Hmax} orientations determined for the San Francisco Bay area and central California and support the hypothesis that the San Andreas fault slips in response to low resolved shear tractions.

We do not observe a significant earthquake-induced stress rotation in areas of pronounced aftershock activity following the 1992 Landers earthquake. This and a similar result regarding the 1994 Northridge earthquake are consistent with the hypothesis that earthquake stress drops are small relative to the strength of the crust, and—combined with the stress orientation data—reinforce our view that the major active faults in southern California are weak and embedded in an otherwise strong crust.

STRESS ORIENTATIONS ALONG THE SAN ANDREAS

Focal mechanism stress inversion is based upon the assumption that stress is locally homogeneous in a given volume. In other words, spatially distinct focal plane mechanisms may be treated as representative of the same stress tensor. Clearly, the legitimacy of this assumption increases as the region encompassing a suite of focal mechanisms decreases in size. There is a trade-off, however, between reducing the size of a region in order to meet the stress homogeneity assumption, and having enough data in each distinct subregion to obtain a well-constrained inversion result. The most straightforward approach in dealing with this is to specify an *a priori* discretization scale. In practice, given the heterogeneous distribution of seismicity, the chosen scale commonly leads to an under-utilization of densely-spaced data (unnecessarily reducing the reliability of the homogeneity assumption in just those areas where it might be reinforced), or the grouping of widely-spaced data, which potentially undermines the assumption of stress homogeneity in the volume of interest. The compromise

is most acute in regions of complicated faulting, where varying fault orientations and associated seismicity patterns do not necessarily fit conveniently into a regular grid.

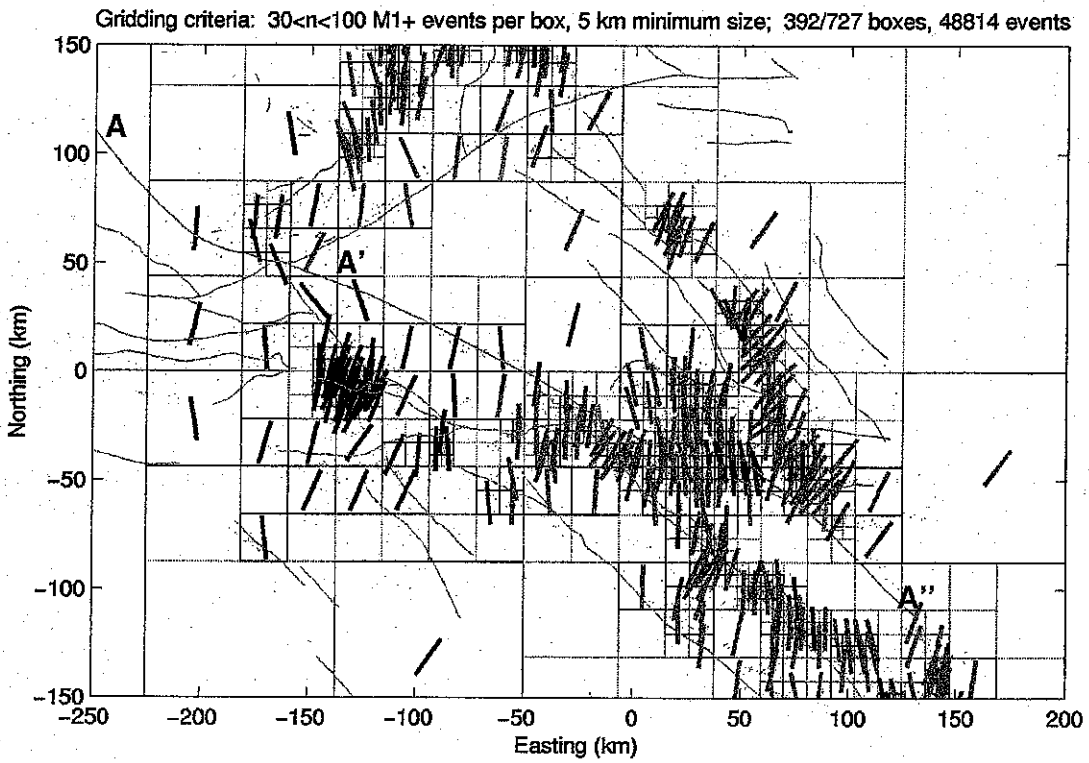

Figure 1: S_{Hmax} orientations and fault patterns in southern California. The grid produced by recursive gridding (with the requirement that each grid cell contain between 30 and 100 focal mechanisms) is illustrated by the gray boxes; dashed boxes do not contain sufficient data for inversion. The black and gray arrows denote strike-slip and reverse stress states respectively. A–A'–A'' is the profile illustrated in Figure 2.

As an alternative, we propose using a data-based recursive method of gridding, which results in a fine grid in areas of dense data, and a correspondingly coarse grid where data are sparse. The advantage of such a method is that it reduces the level of subjectivity required in gridding the data: the grid is controlled by the data locations, and the requirements of the inversion algorithm.

We have adopted this technique in reanalyzing a suite of ~49,000 southern California focal mechanisms previously used by *Hardebeck and Hauksson* (1999) to estimate the orientation of the axis of maximum horizontal compression, S_{Hmax}, along linear cross-sections throughout southern California. As discussed in more detail in *Townend and Zoback* (in press), our motivation has been to determine whether or not the gridding scheme employed by *Hardebeck and Hauksson* (1999) might have influenced their results. In particular, we have reservations about the validity of grouping focal mechanism data into narrow bands as small

as 1 or 2 km (across strike) over distances of as much as ~80 km (along strike) and projecting the resultant stress orientations onto linear profiles in areas of multiple or non-planar faults.

Our results are illustrated in Figure 1 and reveal (1) a high degree of consistency between S_{Hmax} orientations in adjacent cells, (2) a systematically high angle (>60–80°) between S_{Hmax} azimuths and the local strike of the San Andreas and other major faults, and (3) no consistent rotation of S_{Hmax} near major faults at the resolvable scale of 5 km. These results are similar to those obtained by *Provost and Houston* (submitted) within the creeping section of the San Andreas fault northwest of Parkfield, and to the available data in the San Francisco Bay area (*Townend and Zoback*, in press). Figure 2 illustrates near-field stress orientation data—those data points closer than 5 km to the fault trace—along the length of the San Andreas fault in southern California. The mean and standard deviation of the angle between S_{Hmax} and the fault strike are 64° and 14° respectively, indicating that the near-field angle is significantly different at the 95% level of confidence from that obtained by *Hardebeck and Hauksson* (1999) on some of their profiles and later utilized by *Scholz* (2000) to argue for a strong San Andreas on the basis of stress rotations. We do not observe the near-fault S_{Hmax} rotation suggested by *Hardebeck and Hauksson* (1999), and our results are most straightforwardly interpreted as indicating low levels of resolved shear traction on the San Andreas and other faults.

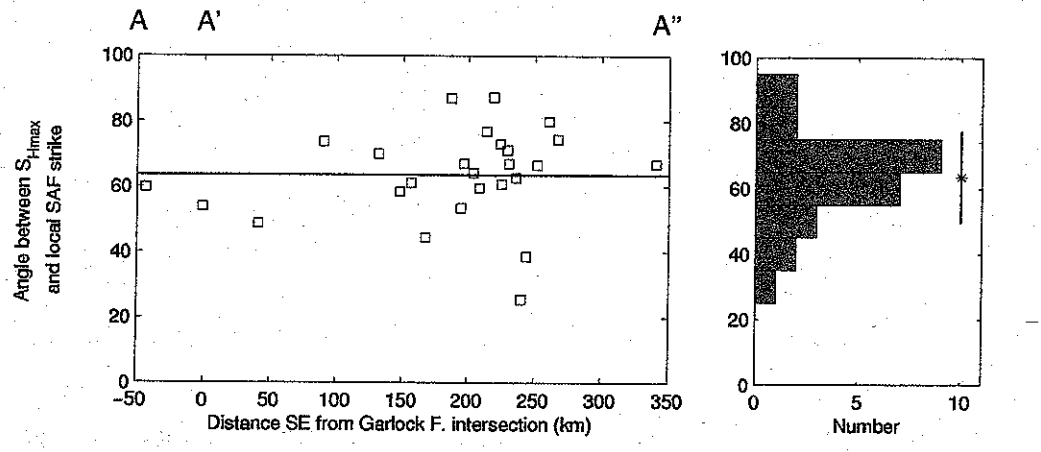

Figure 2: Along-fault profile (left) and histogram (right) of the angle between near-field S_{Hmax} estimates (lying within 5 km of the fault trace) and the local fault strike along the length of the San Andreas fault in southern California (see Figure 1 for profile location). The solid horizontal line indicates the mean angle (64°). In the histogram, the star indicates the mean, and the vertical line illustrates the standard deviation (14°).

STRESS STATE BEFORE AND AFTER LANDERS

We have also applied the recursive gridding methodology to a reinvestigation of whether the 1992 Landers earthquake (M7.2) caused local stress rotation of as much as ~40°, as suggested by *Hardebeck and Hauksson* (1999). We have made the comparison separately inside and outside the zone of pronounced aftershock activity (defined by areas of aftershock activity occurring within 30 days of the Landers mainshock). Where aftershocks did not occur, we presume the stress state to have been relatively unperturbed (the control case),

whereas the occurrence of aftershocks is inferred to indicate a stress perturbation of some sort (the case of interest). Figure 3 illustrates the results of determining stress orientations before ("pre-Landers") and after ("post-Landers") the Landers mainshock and subtracting one set of results from the other. It is immediately apparent that there is little systematic difference in S_{Hmax} azimuth between the two time intervals either inside or outside the aftershock zone.

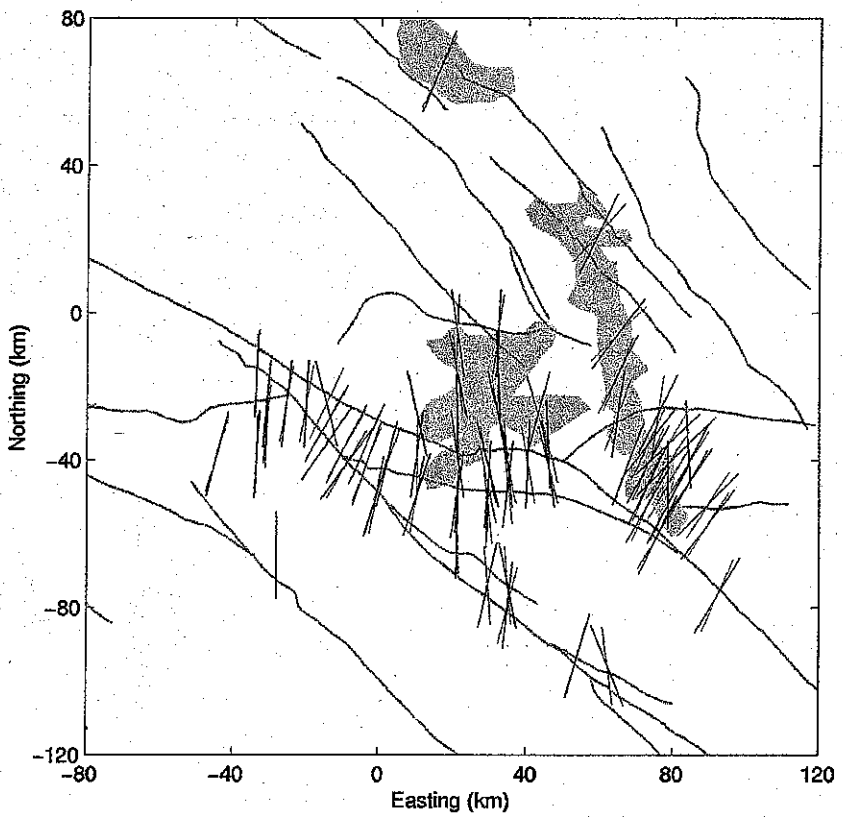

Figure 3: Pre- (black) and post-Landers (gray) S_{Hmax} orientations. The shaded regions indicate zones of pronounced aftershock activity within 30 days of the main Landers event; 86% of the seismicity within this period falls within these zones. Stress orientation data for both the aftershock and control regions are shown quantitatively in Figure 4.

The before and after stress orientation data near Landers are depicted quantitatively in Figure 4. In the control case outside the zone of aftershocks, the histogram of azimuthal differences is clearly centered on zero (mean –0.8°, standard deviation 12.2°, 46 observations), and a t-test indicates that the mean difference is not significantly different from zero at the 95% level of confidence. In the aftershock zone the observed differences (mean 1.4°, standard deviation 12.7°, 19 observations) are not significantly different from zero at the 95% confidence level either. We therefore conclude that our analysis reveals no significant S_{Hmax} rotation induced by the M7.2 Landers earthquake: this is the expected result outside the zone of aftershocks, but somewhat contrary to expectation inside the zone of aftershocks.

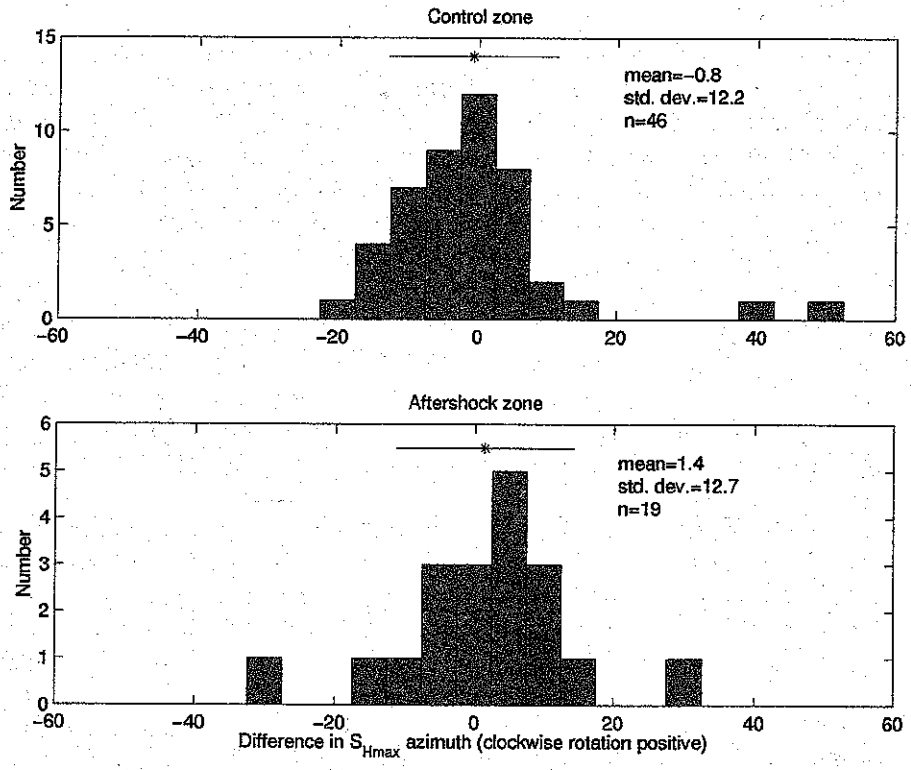

Figure 4: Histograms showing the differences in pre- and post-Landers S_{Hmax} azimuth in the control zone (without appreciable aftershock activity within 30 days of the main rupture; top) and in the aftershock zone (bottom). The data are *post*-Landers azimuth minus *pre*-Landers azimuth; positive values therefore indicate clockwise rotation. All values are in degrees.

Zoback et al. (1987) proposed an expression (rewritten in a slightly simpler format here) relating near-fault stress orientation, α, to fault strength, τ_f, far-field stress orientation, β, and far-field differential stress, ΔS, for an idealized strike-slip fault:

$$\alpha = \frac{\pi}{2} - \frac{1}{2}\tan^{-1}\left[\frac{-2\tau_f}{\Delta S\cos(2\beta)}\right]$$

The far-field strength of planes parallel to the fault is given by $\tau_c=\Delta S\sin(2\beta)$. If we instead interpret τ_c and τ_f as the pre- and post-earthquake fault strengths respectively (so that the earthquake-induced shear stress drop is $\tau_c-\tau_f$) we can use this equation to investigate earthquake-induced stress rotation. In this case β is the pre-earthquake orientation of S_{Hmax} with respect to the fault strike, and $r=\alpha-\beta$ is the stress rotation. For the purposes of this analysis, we envisage the coseismic reduction in shear stress to occur without a change in normal stress, which requires that $45\leq\beta\leq\alpha\leq90°$. The equations for α and τ_c can be combined and rearranged to give

$$\frac{\tau_f}{\tau_c} = \frac{\tan(2\alpha)}{\tan(2\beta)} = \frac{\tan(2\beta + 2r)}{\tan(2\beta)}$$

Given the low fault strength implied by the stress orientation data illustrated in Figures 1–3, and persuasive data showing that crustal differential stress levels are in general substantially higher (e.g. *Townend and Zoback*, 2000), the stress drop remains an even smaller fraction of the *crustal* strength. However, we can estimate both upper and lower bounds on the strength ratio τ_f/τ_c by considering the case of no rotation ($\alpha=\beta\approx70°$, in the vicinity of Landers—Figure 3), and case of maximum rotation consistent with the aftershock zone rotation data. In the case of no rotation, we obtain the trivial result $\tau_f/\tau_c=1$, whatever the value of β. The lower bound on the strength ratio is estimated using a one-sided t-test: for the aftershock zone rotation data in Figure 4, the maximum permissible rotation at the 95% level of confidence is 7.5°, which corresponds to $\tau_f/\tau_c=0.56$ for $\beta=70°$. It is important to recognize that the large standard deviation of the apparent stress rotation observed in the control zone (12°) is probably a reasonable indicator of the measurement uncertainties. If so, it is clear that higher resolution is required to resolve the lower bound on the strength ratio accurately.

The latter point pertains directly to a limitation of currently available stress inversion algorithms. As pointed out by *McKenzie* (1969), one consequence of the conventional assumption of slip in the direction of maximum resolved shear traction (the "Wallace-Bott" hypothesis) is that the only constraint imposed on the stress tensor by an individual focal mechanism is that the axis of maximum compressive stress lie within the dilatational (P) quadrant. Hence, focal mechanisms with similar compressional and dilatational quadrants jointly impose rather weak bounds on the orientation of the stress tensor. An unforeseen outcome of high-resolution earthquake relocation and enhanced data gridding is that it is now possible to grid data, at least locally, with a resolution that produces very low focal mechanism diversity in the smallest cells. Moreover, while *McKenzie's* result implies that the inversion of a low covariance dataset (low focal mechanism diversity) should generate very high model covariance (stress uncertainties), neither of the two most commonly used focal mechanism stress inversion algorithms (*Michael*, 1987a, b; *Gephart*, 1990a, b) appear to appropriately accommodate this. In particular, we have found that small confidence intervals yielded with these techniques often belie very low data covariance and are not representative of the entire range of possible stress tensors.

CONCLUSIONS

Stress orientation data obtained from focal plane mechanism inversions show that within 5 km of the San Andreas fault, the direction of maximum horizontal compression is at a high angle (~64°) to the fault. In apparent contradiction with some of the findings of *Hardebeck and Hauksson* (1999), no large-scale systematic stress rotations of stress orientations are observed near the fault. Rotation of stress orientations to ~45° to the fault were assumed by *Scholz* (2000) in his argument for relatively high frictional strength of the San Andreas. In fact, one would be hard-pressed to identify the location of the San Andreas fault in Figure 1 based on the presumption that such rotations exist. As maximum horizontal stress orientations at high angles to the San Andreas are observed elsewhere along the fault, the general picture that emerges is one of a weak fault in an otherwise strong crust.

Focal mechanism inversions in the vicinity of the Landers earthquake show that the average stress orientation before and after the earthquake is essentially the same, once again in apparent contradiction with the findings of *Hardebeck and Hauksson* (1999). This is true both in the near-field region (characterized by numerous aftershocks) and in the region outside the aftershock zone, for which we utilized pre- and post-earthquake focal plane mechanism inversions as a control group. This indicates that the stress drop in the earthquake was much smaller than the stress driving the earthquake. However, in both the aftershock zone and the control area, there is relatively large scatter in the pre- and post-Landers stress orientations (~12.5°) making it difficult to resolve any small-scale changes.

REFERENCES

Gephart, J.W., Stress and the direction of slip on fault planes, Tectonophysics, 9, 845–858, 1990a.

Gephart, J.W., A Fortran program for inverting fault/slickenside and earthquake focal mechanism data to obtain the regional stress tensor, Computers and Geosciences, 16, 953–989, 1990b.

Hardebeck, J.L., E. Hauksson, Role of fluids in faulting inferred from stress field signatures, Science, 285, 236–239, 1999.

Hauksson, E., Crustal structure and seismicity distributions adjacent to the Pacific and North America plate boundary in southern California, Journal of Geophysical Research, 105, 13875–13903, 2000.

McKenzie, D.P., The relation between fault plane solutions for earthquakes and the directions of the principal stresses, Bulletin of the Seismological Society of America, 59, 591–601, 1969.

Michael, A.J., Determination of stress from slip data: faults and folds, Journal of Geophysical Research, 89, 11517–11526, 1987a.

Michael, A.J., Use of focal mechanisms to determine stress: a control study, Journal of Geophysical Research, 92, 357–368, 1987b.

Provost, A.-S., H. Houston, Orientation of the stress field surrounding the creeping section of the San Andreas fault: evidence for a narrow mechanically weak fault zone, Journal of Geophysical Research, submitted.

Scholz, C.H., Evidence for a strong San Andreas fault, Geology, 28, 163–166, 2000.

Townend, J., M.D. Zoback, How faulting keeps the crust strong, Geology, 28, 399–402, 2000.

Townend, J., M.D. Zoback, Implications of earthquake focal mechanisms for the frictional strength of the San Andreas fault system, Special Publication of the Geological Society of London, in press.

Zoback, M.D., M.L. Zoback, V.S. Mount, J. Suppe, J.P. Eaton, J.H. Healy, D. Oppenheimer, P. Reasenberg, L. Jones, C.B. Raleigh, I.G. Wong, O. Scotti, C. Wentworth, New evidence on the state of stress of the San Andreas fault system, Science, 238, 1105–1111, 1987.